

Evaluation of drug loading capacity and release characteristics of PEDOT/naproxen system: effect of doping ions

Katarzyna Krukiewicz^{a,b,*,**}, Aleksandra Kruk^a, Roman Turczyn^a

^aDepartment of Physical Chemistry and Technology of Polymers, Silesian University of Technology, Strzody 9, 44-100 Gliwice, Poland

^bCentre for Research in Medical Devices (CURAM), Galway Biosciences Research Building, 118 Corrib Village, Newcastle, Galway, Ireland

* corresponding author

Department of Physical Chemistry and Technology of Polymers, Silesian University of Technology, Strzody 9, 44-100 Gliwice, Poland

katarzyna.krukiewicz@polsl.pl

** ISE member

Abstract

Conducting polymers are versatile and robust materials that have recently become attractive as controlled drug delivery systems. Possessing ion exchangeable properties, they can serve as carriers for numerous biologically active species, showing particular applicability in neural tissue engineering and regional chemotherapy. In the pursuit of the design of the most effective controlled drug delivery system, we aimed to compare the performance of the conducting polymer-based matrix as a function of doping anion, using chloride, perchlorate and dodecyl sulfate, respectively, as the primary dopants. Due to their different ion radius and mobility, selected ions were found to provide substantial changes into polymer characteristics, having strong effects into the uptake and release of a model drug, naproxen sodium salt. PEDOT/CIO₄ matrix, particularly, was found to possess superior properties providing highest mass of the formed polymer ($103.45 \pm 10.09 \mu\text{g cm}^{-2}$), charge storage capacity (44.9 mC cm^{-2}) and ion exchange capacity ($0.122 \pm 0.003 \mu\text{mole cm}^{-2}$), leading also to the highest amounts of loaded ($0.024 \pm 0.002 \mu\text{mol cm}^{-2}$) and released (from $0.71 \pm 0.10 \mu\text{g cm}^{-2}$ to $1.61 \pm 0.59 \mu\text{g cm}^{-2}$) drug.

Keywords

conducting polymers; controlled drug delivery; drug loading capacity; electrochemical quartz crystal microbalance; naproxen

1. Introduction

Conducting polymers, due to their versatility and tunable properties, have already found numerous potential applications in a variety of fields. Apart from serving as materials for organic solar cells [1,2], light emitting diodes [3,4] or electrochromic devices [5,6], conducting polymers are also often considered as materials suitable for biomedical purposes, such as drug delivery systems (DDS) [7,8]. Possessing ion exchangeable properties, they can serve as carriers for numerous charged biologically active species, such as antibiotics [9,10], anti-inflammatory drugs [11,12] and anti-cancer agents [13,14], showing particular applicability in neural tissue engineering and regional chemotherapy. The ability to release immobilized molecules in a response to electrical stimulation is an additional benefit allowing conducting polymers to be used as controlled DDS [15].

Apart from typical chemical synthesis, conducting polymers can be obtained in a course of electrochemical polymerization. Electropolymerization has been found to be a highly controllable technique, in which by the careful choice of process parameters it is possible to tailor the properties of the resulting material to specific needs. Among numerous technical parameters, such as the oxidation potential, current density and scan rate, also the choice of a doping ion can be used to adjust such properties as conductivity and surface morphology [16–18]. Since these properties are also supposed to influence drug loading capacity of conducting polymers and their reaction to stimulating potential, it is expected that the choice of a doping ion should have a significant impact on the performance of conducting polymer-based DDS.

Up to date, a few electrolytes have been used as primary dopants for the formation of conducting polymer-based DDS. The requirements for an efficient conducting matrix are focused on two major properties, i.e. high conductivity [19] and biocompatibility [20–25]. The latter can be relatively easily fulfilled when the biologically inert, small ions are used as primary dopants; the most popular example is Cl^- [13,26]. One of the recent concepts includes the use of dopants possessing biological functionality, e.g. dexamethasone [11] or ibuprofen [15]. Although the incorporation of these molecules in the step of matrix formation can be beneficial from the biological point of view, it could also result in the formation of less conductive, thin deposits with limited stability [15]. The alternative concept is to use a three step drug loading process, when the matrix is first formed in the presence of doping ions known from providing polymers with remarkably high conductivity, and the drug loading occurs in the following ion exchange process. The most effective primary dopants are the electrolytes possessing large ions, such as sodium p-toluenesulfonate (PTS) and poly(sodium 4-styrenesulfonate) (PSS). Polymer matrices formed in the presence of PTS and PSS have been found as highly biocompatible and superior in terms of high conductivity [27–29]. The major disadvantage is, however, the limited mobility of PTS and PSS within the polymer matrix, which, from the point of view of a drug delivery system, is essential since the basis of the drug release is the ion exchange process.

In the pursuit of the design of the most effective DDS, we aimed to compare the performance of a conducting polymer-based matrix as a function of a doping ion size. In this

study, we have compared the drug loading efficiency as well as release characteristics of poly(3,4-ethylenedioxythiophene), PEDOT, matrix formed in the presence of three electrolytes, namely KCl, LiClO₄ and sodium dodecyl sulfate (C₁₂H₂₅SO₄Na, DS). The ionic radii of Cl⁻ and ClO₄⁻ are 181 pm and 240 pm, respectively [30], while DS in aqueous solution forms micelles with average radius of 2.2 μm [31,32]. These dopants, due to their different molecular size and mobility within polymer matrix, are supposed to provide substantial changes into polymer characteristics, having its effects into the loading and release of a model drug, naproxen sodium salt (NPX). The three step drug loading method was applied to fabricate the drug-loaded matrices, consisting of the matrix fabrication in the presence of primary dopant, followed by the electrochemical removal of primary dopant and electrochemical drug loading [10]. For the release experiments, both potentiostatic and potentiodynamic modes were used, comprising spontaneous, chronoamperometric and cyclic voltammetric release protocols. In order to provide quantitative results, the electrochemical quartz crystal microbalance (EQCM) was employed to monitor these processes *in situ*.

2. Materials and Methods

2.1 Matrix formation

Conducting polymer matrices were synthesized through the electrochemical oxidative polymerization by means of CHI 400c Electrochemical Workstation equipped with the time-resolved electrochemical quartz crystal microbalance. Standard three-electrode setup was used, employing CHI 125 gold crystal (0.205 cm²) as a working electrode, Ag/AgCl (3M KCl) as a reference electrode ($E = 0.205$ V *vs.* SHE) and a platinum foil (1 cm²) as a counter electrode. The electrochemical polymerization of 3,4-ethylenedioxythiophene (EDOT, 97 %, Sigma Aldrich) (10 mM) was performed with the use of a cyclic voltammetry, in which the potential was swept between -0.5 V and 1.1 V or 1.2 V (*vs.* Ag/AgCl), at a scan rate of 0.1 V s⁻¹, for 25 potential cycles in 0.1 M KCl (99 %, Sigma Aldrich), 0.1 M LiClO₄ (99.99 %, Sigma Aldrich) or 0.1 M C₁₂H₂₅SO₄Na (DS, 99 %, Sigma Aldrich) aqueous solutions, respectively.

2.2 Drug loading

(S)-6-Methoxy- α -methyl-2-naphthaleneacetic acid sodium salt (Naproxen, NPX, 98 %, Sigma Aldrich) was chosen as a model drug. NPX loading was performed by means of an ion exchange process, in which the previously synthesized PEDOT matrix was first dedoped to remove the primary dopant (KCl, LiClO₄ or DS), and then reoxidized in the presence of NPX. Dedoping of the polymeric deposit was achieved in 0.1 M KCl, 0.1 M LiClO₄ or 0.1 M DS solutions, respectively, at a constant working electrode potential of -0.5 V (*vs.* Ag/AgCl) over 600 s. NPX loading was carried out by the potentiostatic doping of PEDOT at 0.5 V (*vs.* Ag/AgCl) in 0.1 M NPX aqueous solution for 600 s.

2.3 Electrochemical characterization

The electrochemical properties of PEDOT matrices formed in the presence of three different primary dopants, namely Cl^- , ClO_4^- and $\text{C}_{12}\text{H}_{25}\text{SO}_4^-$, were characterized by means of a cyclic voltammetry (Gamry Reference 600 potentiostat). CV curves were collected in 0.1 M KCl solution in the potential range between -0.5 V and 0.9 V (*vs.* Ag/AgCl), at a scan rate of 0.1 V s^{-1} , for 3 potential cycles. Cyclic voltammograms were used to determine the charge storage capacity (CSC), calculated as the electric charge integrated under corresponding CV curve during one CV cycle [15]. The measurements were performed in triplicate, the results were expressed as a mean \pm standard deviation. The degree of doping was determined as the number of counteranions per monomer unit of the conducting polymer.

Electrochemical impedance spectra were collected by means of a PARSTAT 2273 potentiostat in 0.1 M KCl solution within a frequency range from 100 mHz to 5 kHz, with AC amplitude of 40 mV (*vs.* Ag/AgCl) and DC potential equal to 0 V (*vs.* Ag/AgCl). The results were presented on Bode plots and compared to those of bare Pt electrode. The data fitting analysis was performed using EIS Spectrum Analyzer 1.0 software with the application of Powell algorithm.

2.4 Chemical and morphological characterization

SEM images were collected by means of Hitachi S-4700 Scanning Electron Microscope operating at 5 kV. Surface morphology was analyzed with the use of a Phenom Pro-X Scanning Electron Microscope and 3D Roughness Reconstruction software. IR spectra were recorded using Varian 660-IR FT-IR Spectrometer in the range between 4000 and 600 cm^{-1} for 16 scans.

2.5 Drug release

The release experiments were conducted in a phosphate buffer saline 1x solution (PBS, Sigma Aldrich) and monitored *in situ* by a time-resolved EQCM (CHI 400c with CHI125 gold crystal electrode). Spontaneous release was carried out under open circuit conditions for 600 s, while active release was performed by applying a negative potential of -0.5 V (*vs.* Ag/AgCl) for 600 s (CA mode) or by means of cyclic voltammetry in the potential range between -0.5 V and 0.5 V (*vs.* Ag/AgCl), at a scan rate of 0.1 V s^{-1} for 30 potential cycles within 600 s (CV mode). The measurements were performed five times and the results were expressed as a mean \pm standard deviation. The amounts of released NPX were confirmed with the use of UV-Vis spectrophotometry (Hewlett Packard 8453 UV-Vis Diode Array Spectrophotometer), and based on the absorbance at the characteristic for NPX peak (272 nm) [33] (Fig.S1). The release kinetics was analyzed with the use of Avrami's equation:

$$X = 1 - \exp(-kt^n)$$

and its linear form:

$$\ln(-\ln(1 - X)) = \ln k + n \ln t$$

where: X is the fraction of drug released at time t , n is the Avrami parameter and k is the release rate constant [34].

2.6 Mass change calculations

The change of mass of a quartz crystal was calculated based on the frequency change (Δf) as given by the Sauerbrey equation:

$$\Delta f = \frac{-2f_0^2}{A(\mu\rho)^{1/2}} \Delta m$$

where f_0 is the resonant frequency of the fundamental mode of the crystal, A is the area of the gold crystal working electrode (0.205 cm^2), ρ is the density of the crystal (2.648 g cm^{-3}) and μ is the shear modulus of quartz ($2.947 \cdot 10^{11} \text{ g cm s}^{-2}$). For 8 MHz crystal used in this work, a 1 Hz change in frequency corresponded to the mass change of 1.4 ng. The measurements were performed in triplicate, the results were expressed as a mean \pm standard deviation.

3. Results and Discussion

3.1 Electrochemical polymerization of EDOT

The three step drug loading method supports the fabrication of conjugated polymer matrices with enhanced electrochemical properties, since the parameters of electrochemical polymerization process can be better optimized in the absence of drug molecules in the reaction system [15]. This method also allows to load drugs which could be unstable at the high positive potentials, as in case of naproxen, for which the irreversible oxidation starts at the potential as low as 0.8 V vs. Ag/AgCl (Fig.S2) [35]. Cyclic voltammograms collected during the electropolymerization of EDOT (Figure 1A-C) present the typical constant increase in the current passing through the electrode, confirming the formation of a conductive deposit. Also the constant rate of the mass increase, corresponding with the increase in charge passing through the electrode (Figures 1D-F), confirms that the process of electropolymerization and polymer deposition proceeds with no traces of the undesirable overoxidation nor degradation of formed polymer film. The additional reduction signal that is observed at the potential of 0.5 V vs. Ag/AgCl in the CV curve of the electrochemical polymerization of EDOT in the presence of Cl⁻ should be associated with the reduction of gold that was beforehand partially oxidized at the potentials required for the formation of polymer. The similar occurrence of a gold electrode oxidation and reduction processes has

been already described in the literature [36,37]. The expected oxidation peak of gold is not observed because of its overlapping with signal derived from the oxidation of EDOT.

The major difference among performing the electropolymerization processes in the presence of various electrolytes is the overall mass of the polymer. For the same number of CV cycles, 2.5 times more polymer is deposited in the presence of LiClO_4 ($103.45 \pm 10.09 \mu\text{g cm}^{-2}$) than KCl ($42.07 \pm 2.53 \mu\text{g cm}^{-2}$), which is in agreement with the counter ion affinity described in [30,38] and follows the general trend suggested by the Hofmeister series [39]. In short, the weak hydration of ClO_4^- in comparison to Cl^- may be the reason why ClO_4^- interacts stronger with PEDOT and acts easier as the counter ion during electropolymerization [40].

The lowest amount of polymer was formed in the presence of DS as a dopant ($17.49 \pm 0.58 \mu\text{g cm}^{-2}$). This can be only partially explained by the difference in the molecular mass of primary dopants, since all of them are monovalent and if the rates of polymer formation are the same, the highest mass is expected for the PEDOT/DS system. The opposite observation indicates the inhibitory effect of DS on the electropolymerization of EDOT, which can be explained by the adsorption of the surfactant molecules on electrode/electrolyte and polymer/electrolyte interface resulting in the modification of surface characteristics and electron transfer effectiveness [41]. These phenomena lead to the decrease in the rate of film formation in a similar way as it was reported in case of other surfactants, e.g. Tween 80, which inhibited the oxidation of aniline [42].

Here Figure 1

Apart from influencing polymerization efficiency, the choice of dopant has also the effect on inherent electrochemical performance of formed polymer (Figure 2A-C), i.e. charge transfer characteristics. In general, there are two types of materials used for neural interfaces, namely materials experiencing faradaic reactions that mediate the flow of electrons, and capacitive materials experiencing charging and discharging of the electrode-electrolyte double layer [43]. It occurs very often that a mechanism of charge transfer is mixed, exhibiting both electron and ion transport within the bulk of the coating. Providing that the electrode material is stable during electrical stimulation, there is no preferred mechanism of charge transfer. Therefore, it is not necessary to distinguish between capacitive, faradaic and background currents.

Undoubtedly, it is the CV of PEDOT/ ClO_4 that is characterized by the most developed shape and the highest charge storage capacity defined as the area under the CV curve ($\text{CSC} = 44.9 \text{ mC cm}^{-2}$). CSC of PEDOT/ ClO_4 is two times higher than for PEDOT/ Cl (21.2 mC cm^{-2}) and almost seven times higher than for PEDOT/DS (6.6 mC cm^{-2}), proving its efficiency in providing the high charge transfer area [44] and indicating its applicability as a neural interface [45]. The effect of the doping ion on the impedance of polymer is clearly observed when EIS spectra of PEDOT/ Cl , PEDOT/ ClO_4 and PEDOT/DS are compared (Fig.1C). To

determine the values of the conductivities of PEDOT, the experimental data were fitted to a simple Randles circuit (inset in Fig.2C), which is composed of a solution resistance (R_s), charge transfer resistance (R), constant phase element (CPE) and Warburg diffusion element (W) [46]. The simulated data show that the lowest resistance is exhibited by PEDOT/Cl ($29.5 \pm 4.8 \Omega$), and it increases for PEDOT/DS ($94.9 \pm 5.9 \Omega$) and PEDOT/ClO₄ ($280.1 \pm 64.1 \Omega$). The significant decrease in the solution resistance (R_s) for the latter ($371.0 \pm 4.2 \Omega$), when compared with both PEDOT/Cl and PEDOT/DS ($961 \pm 13.2 \Omega$ and $975 \pm 2.7 \Omega$, respectively) indicates that the ion exchange between matrix and electrolyte solution occurs even for the mild potential stimulation (± 40 mV *vs.* Ag/AgCl). This is also supported by the values of a Warburg diffusion constant which reaches the highest value for PEDOT/ClO₄ (Table S1).

The mobility of doping ions within a polymer matrix plays a crucial role in the step of drug loading, since this process is based on the ion exchange between conducting polymer matrix and solution [47]. Therefore, the total drug loading capacity of the matrix can be assessed by analyzing mass changes occurring within the oxidation-reduction cycles (Figure 2A-B). Also here, the highest mobility of ClO₄⁻ is the cause of the most pronounced mass change of the polymer film (deposited on electrode) (Table 1), corresponding with the superior ion exchange capacity of $0.122 \pm 0.003 \mu\text{mole cm}^{-2}$, and being in good agreement with the previous studies [48]. Although the mass changes for both PEDOT/Cl and PEDOT/DS seem to be similar, due to the differences in molecular masses of both dopants this is PEDOT/Cl matrix that is characterized with higher ion exchange capacity than PEDOT/DS, and only 47 % lower than PEDOT/ClO₄. It is worth to note that the estimated ion exchange capacity is the maximum theoretical amount of ion, either primary dopant or secondary one (molecules of a drug), which can be loaded during the ion exchange process. The actual amount of a loaded drug is dependent on the several additional factors, among which the mutual correlation between the size of a drug molecule and the size of a leaving primary dopant seems to play an important role.

Here Figure 2 & Table 1

3.2 Electrochemical loading of NPX

In order to remove the primary doping ions, the as-formed PEDOT matrices were subjected to a potential of -0.5 V (*vs.* Ag/AgCl). The mass change *vs.* time curve, associated with this process (Figure 3A) shows that 600 seconds was enough to reach a plateau indicating complete ion removal. It is worth to note that the amounts of primary dopant removed in this step are lower than the ion exchange capacities determined earlier in this study. This is caused by the fact that the process of electropolymerization was designed to finish at a lower vertex potential, hence the as-formed matrix was already in a partially reduced state and the amount of primary dopant was also lower. According to the mass of the polymer matrix fabricated in the presence of different dopants, as well as the mass decrease due to the removal of dopant

(Table 2), the degree of doping was determined as 0.048 ± 0.007 for PEDOT/Cl, 0.023 ± 0.004 for PEDOT/CIO₄ and 0.007 ± 0.001 for PEDOT/DS.

In the last step of the drug loading procedure, neutral PEDOT matrices were immersed in 0.1 M NPX solution and subjected to the potential of +0.5 V (vs. Ag/AgCl). The highest rate of mass increase, equivalent to the highest rate of drug loading, was observed in the first 20 s of doping process for both PEDOT/Cl and PEDOT/DS, and for 30 s longer in case of PEDOT/CIO₄ (Figure 3B). After 600 s of the application of a positive potential, the mass of the latter was still increasing, reaching the plateau after 950 s, confirming its superior ion exchange capacity. The highest achieved drug loading capacity is expressed by PEDOT/CIO₄ and is equal to $0.024 \pm 0.002 \mu\text{mol cm}^{-2}$. It is substantially higher than for both PEDOT/Cl ($0.011 \pm 0.001 \mu\text{mol cm}^{-2}$) and PEDOT/DS ($0.005 \pm 0.001 \mu\text{mol cm}^{-2}$). Nevertheless, in all cases the estimated drug loading capacities are much lower than the maximum theoretical loading capacities, showing that NPX can substitute the primary dopant only partially during the last step of proposed drug loading procedure. Surprisingly, when the amount of loaded NPX is calculated with respect to the total mass of polymer matrix (Table 2), the drug content is in the range between 5-6 wt% regardless of the primary doping ion, and the differences among all polymers are statistically insignificant. Consequently, the type of a dopant is confirmed to play the major role in the process of matrix formation, being able to enhance or suppress the electropolymerization process. Drug loading capacity, however, is found to be the intrinsic property of the polymer, and dependent on the electrostatic interactions between charged matrix and drug ions, with the negligible effect of the doping ion.

Here Figure 3 & Table 2

3.3 FTIR characterization

The three step drug loading method is a technique in which drug is located mainly in the near surface layers of matrix [13]. Therefore, the presence of signals corresponding to NPX is expected in the FTIR spectrum of drug-loaded PEDOT. The FTIR spectrum of NPX (Figure 4) is characterized by the bands associated with ring deformation (686 cm^{-1} , 924 cm^{-1} and 1264 cm^{-1}), ring stretching (746 cm^{-1}), ring bending (815 cm^{-1} , 855 cm^{-1} and 888 cm^{-1}), C-H ring bending (1025 cm^{-1} , 1060 cm^{-1} , 1161 cm^{-1} and 1387 cm^{-1}), as well as C-C ring stretching (1604 cm^{-1} and 1631 cm^{-1}) [49]. FTIR spectrum of PEDOT, on the other hand, is characterized by the presence of bands associated with C-C and C=C stretching in thienylene moiety (1472 cm^{-1} and 1382 cm^{-1}), ethylenedioxy unit stretching (1079 cm^{-1}) as well as C-S vibrations (925 cm^{-1}) and C-S-C deformation (711 cm^{-1}) [50–52].

The FTIR spectra of drug-loaded PEDOT exhibit high similarity to the spectra of pristine PEDOT, but also evidence of the presence of NPX molecules in polymer matrix is confirmed by the occurrence of characteristic for this drug bands. For PEDOT/Cl-NPX, these are the bands corresponding to the in plane C-H ring bending (1060 cm^{-1}) and in plane ring

deformations (924 cm^{-1}). In the spectrum of PEDOT/ ClO_4 -NPX, the peaks characteristic for NPX are present at 1025 cm^{-1} (C-H bending) and 746 cm^{-1} (in plane ring stretching); the signals at 1264 cm^{-1} (in plane C-C ring deformations) and 686 cm^{-1} (out of plane ring deformation) confirm the presence of NPX in PEDOT/DS-NPX. The other characteristic peaks, especially those associated with aromatic rings, are indistinguishable with the signals coming from the polymer matrix backbone.

Here Figure 4

3.4 Surface morphology

Numerous studies have already confirmed the major influence of the polymerization conditions on the surface morphology of conducting polymer layers [53,54]. Also in our study, the alteration in the primary dopant resulted in the formation of PEDOT with significantly different morphology, as shown in SEM images of pristine and NPX-loaded PEDOT/Cl, PEDOT/ ClO_4 and PEDOT/DS matrices (Figure 5A-F). The corresponding distribution of diameters of grain-like structures is shown in Figure 5G in a form of histograms. The most uniform is undoubtedly the surface of PEDOT/Cl, in case of both the pristine and NPX-loaded matrix, with the majority of the grain diameters distributed between $0.1\text{ }\mu\text{m}$ and $3\text{ }\mu\text{m}$, and the average grain diameter of $1.76 \pm 0.70\text{ }\mu\text{m}$ (PEDOT/Cl) and $0.26 \pm 0.07\text{ }\mu\text{m}$ (PEDOT/Cl-NPX), which is typical for EDOT polymerized in the presence of small dopants [55]. Although uniform, this matrix is characterized by quite high roughness ($S_a = 936\text{ nm}$), which is further reduced by the removal of Cl ($S_a = 584\text{ nm}$) and almost unchanged when PEDOT/Cl is loaded with NPX ($S_a = 565\text{ nm}$) (Fig.S3). Since the surface morphology is related to the porosity of polymer matrix, i.e. availability of the interstitial pore, smaller grains indicate more compact structure which could limit the future accessibility of the polymer during the drug loading stage and also block the release of drug, especially if the size of a drug molecule is larger than the size of primary dopant.

In contrast to PEDOT/Cl, the surface of PEDOT/ ClO_4 is covered with circular features with a characteristic doughnut shape, particularly visible for NPX-loaded matrix. The features of this shape has been already observed not only for PEDOT/ ClO_4 [56], but in general for a template-assisted polymerization of EDOT [57,58], and may result from the strong interactions between EDOT and ClO_4^- explained by the position of this dopant in the Hofmeister series. The average diameter of these features is larger than in case of PEDOT/Cl, and equals to $3.46 \pm 0.99\text{ }\mu\text{m}$ and $4.29 \pm 2.02\text{ }\mu\text{m}$ for pristine and drug-loaded PEDOT/ ClO_4 , respectively. The increase in the grain diameter, which is assisted by the increase in roughness (S_a of 406 nm and 684 nm for the pristine and NPX-loaded matrix, respectively), is simply caused by the incorporation of bulky ClO_4^- (ionic radius of 240 pm [30]) instead of Cl (ionic radius of 181 pm [30]), and is consistent with previous literature reports, e.g. for polyaniline [59] and polypyrrole [60].

The surface of PEDOT/DS, on the other hand, is covered with the cell-shaped features which are uniformly distributed over the whole area of the electrode. The average diameter of the polymer grains is equal to $5.05 \pm 1.38 \mu\text{m}$ and $4.19 \pm 1.25 \mu\text{m}$ for pristine and drug-loaded PEDOT/DS, respectively. The regular shape of these features is expected to result from the presence of DS micelles [31,32] serving as a template for the growing polymer chain to form ordered surfactant-templated conducting polymer matrices [61], similarly to PEDOT grown in the presence of other surfactants [62]. NPX loading is not shown to have a significant impact on the surface morphology of PEDOT/DS, with the roughness only slightly increased from S_a of 622 nm for PEDOT/DS to S_a of 754 for PEDOT/DS-NPX. Nevertheless, the evident variations in the surface morphology among PEDOT/Cl, PEDOT/ClO₄ and PEDOT/DS, resulting from different dopant nature and size, are supposed to reflect in the alteration in drug release characteristics, that will be extensively discussed in the next section.

Here Figure 5

3.5 Spontaneous release

Conducting polymers are well known for their ability to release drug molecules in a response to the electrical trigger. Nevertheless, they are still able to release drugs spontaneously, without the application of external stimulus [7]. Determination of the ratio of the amount of drug released in these two mechanisms allows to differentiate between drugs interacting strongly or weakly with the matrix. The amounts of NPX that were spontaneously released from the various PEDOT matrices, shown in Figures 6A&7 and Table 3, were found to be the highest for PEDOT/ClO₄ (39 % of total drug content), but still substantial for both PEDOT/Cl (33 %) and PEDOT/DS (27 %). Interestingly, this is also close to the order of the ion exchange capacity of matrices, suggesting that the high mobility of the primary dopant within polymer matrix can be partially responsible for the increased drug availability. Even though the control of the release is highly desired, the initial burst release can be beneficial, e.g. in neural tissue engineering, where high quantities of drugs can be used to treat acute inflammatory states accompanying the processes of neural probe implantation [27,63]. If conducting polymers are going to be used in this way, however, the spontaneous release must be well characterized and tailored in order to possess the desired kinetics.

Numerous mathematical models can be applied to describe the release kinetics, however this is Avrami's model that is the most frequently used for conducting polymer-based drug delivery systems [14,33,34,64,65]. The results of spontaneous release of NPX were fitted with Avrami's kinetics model in a function of time. The release kinetic parameters are presented in Table S2 and the fitted release curves are plotted together with the experimental curves in Fig. 6A. The data show that the highest rate constant of a spontaneous release (0.012 s^{-1}), as expected, is observed for PEDOT/ClO₄, outperforming both PEDOT/Cl (0.010 s^{-1}) and PEDOT/DS (0.002 s^{-1}), as well as other conducting polymer-based systems, e.g. salicylate-loaded polypyrrole [34] and methotrexate-loaded polypyrrole [14]. The values of the

Avrami's exponent (n parameter) approaching 1 indicate that the spontaneous release of NPX from PEDOT matrices, especially PEDOT/Cl, represents a first-order kinetics and the mechanism of release occurs through a complex transport rather than a pure diffusion [14].

3.6 Electrically-triggered release

The most important from the point of view of controlled drug delivery is the possibility to design an electrically-triggered DDS. Among numerous modes of electrical stimulation, two are considered as the most effective, namely constant potential application (chronoamperometric release, CA) and cyclic potential sweep (cyclic voltammetric release, CV). CA approach is based on the removal of anionic drug through the application of a negative potential, in a similar way as it has been done for the removal of primary dopant. Since the electrostatic interactions between the positively-charged polymer matrix and negatively-charged dopant are responsible for the drug loading, the changing of the matrix state as well as the force vector direction from attraction into repulsion can be used to trigger the drug release [34]. Well-described contraction of conducting polymer upon the application of negative potential, that has the effect in surface morphology of matrices (Fig.S3), is the other factor that control the release of drug [66]. The most crucial parameter here is the magnitude of potential, which should be high enough to cause a drug release but not too high to cause degradation. It has been also observed that the matrix subjected to excessively negative potentials may start to uptake cations from the electrolyte solution instead of releasing anionic dopant [15]. Consequently, the most efficient release potential for PEDOT was determined to be equal to -0.5 V (vs. Ag/AgCl). Under these conditions, the highest drug amount is released from PEDOT/CIO₄ ($0.71 \pm 0.10 \mu\text{g cm}^{-2}$), which is only 13 % of the total drug content (Figures 6B&7 and Table 3). The highest percentage of the total drug content released in CA mode is noted for PEDOT/DS (25 %), but because of the low drug loading capacity of PEDOT/DS, it corresponds to only $0.28 \pm 0.06 \mu\text{g cm}^{-2}$ of NPX. Although low concentrations of NPX, the release of drug from PEDOT/DS is observed to be the most linear among all investigated matrices ($R^2 = 0.994$ between 150 s and 600 s), with the release rate constant of 0.104 s^{-1} , which is much higher than for similar conducting polymer-based drug delivery systems described in the literature [14,33], showing that a short electrical stimulus is enough to achieve therapeutically relevant drug doses. Interestingly, the amount of NPX loaded in an irreversible manner is the same for all types of matrices, and is equal to approx. 48 %, suggesting that the amount of released NPX is limited by the residual charges within the PEDOT matrix [67], that is the intrinsic property of the polymer with the negligible effect of the primary dopant.

Here Figure 6

In recent studies [68,69], CA mode of release is often replaced by CV, which provides milder conditions of the ion exchange process. In contrast to CA, where the matrix is continuously subjected to a negative potential, CV allows the matrix to be repetitively reduced and oxidized enabling to work at the equilibrium state and to use electrolyte ions for the neutralization of a polymer charge. Also in CV mode the highest amount of drug is released from the PEDOT/CIO₄ matrix ($1.61 \pm 0.59 \mu\text{g cm}^{-2}$), which stands for 29 % of the total drug content (Figures 6C&7 and Table 3). This matrix is also characterized by the highest release rate constant (0.069 s^{-1}). Once again, the highest percentage of the total drug content released in CV mode (53 %) is typical for PEDOT/DS ($0.58 \pm 0.08 \mu\text{g cm}^{-2}$ of NPX). Except from PEDOT/Cl, for which the amount of NPX released in CA is slightly higher than for CV, cyclic voltammetric mode is confirmed as the most efficient electrical trigger resulting in the decrease of the wt% of NPX permanently loaded down to 20 % (PEDOT/DS) and 32 % (PEDOT/CIO₄). The high amount of NPX permanently loaded in PEDOT/Cl is supposed to result from the most dense surface morphology of this matrix, as it was discussed in the previous section.

Here Figure 7 & Table 3

4. Conclusions

In order to design the most effective DDS, we aimed to compare the performance of PEDOT matrix as a function of the doping ion size using Cl⁻, ClO₄⁻ and C₁₂H₂₅SO₄⁻ as primary dopants. The major difference among performing the electropolymerization in the presence of various electrolytes was the overall mass of the formed polymer, being the highest for LiClO₄ ($103.45 \pm 10.09 \mu\text{g cm}^{-2}$) and the lowest for DS ($17.49 \pm 0.58 \mu\text{g cm}^{-2}$). PEDOT/CIO₄ matrix was also characterized by the highest charge storage capacity (44.9 mC cm^{-2}) and ion exchange capacity ($0.122 \pm 0.003 \mu\text{mole cm}^{-2}$), leading also to the highest amount of loaded drug, NPX ($0.024 \pm 0.002 \mu\text{mol cm}^{-2}$). The type of dopant was confirmed to play the major role in the process of matrix formation, being able to enhance or suppress the electrochemical polymerization. Drug loading capacity, however, was found to be the intrinsic property of the polymer, and dependent on the electrostatic interactions between charged matrix and drug ions.

The release experiments showed that the amount of NPX released spontaneously was dependent on the ion exchange capacity of matrices, suggesting that the high mobility of primary dopant should be considered as responsible for the increased drug availability. For both chronoamperometric and cyclic voltammetric release modes, it was the PEDOT/CIO₄ matrix that was found out to be able to release the highest amount of NPX, $0.71 \pm 0.10 \mu\text{g cm}^{-2}$ and $1.61 \pm 0.59 \mu\text{g cm}^{-2}$, respectively. It was, however, PEDOT/DS which allowed the most controlled delivery of NPX, although the amounts of NPX were much lower than in case of the other matrices. Except from PEDOT/Cl, for which the amount of NPX released in CA was slightly higher than for CV, cyclic voltammetric mode was found as the most efficient

electrical trigger allowing the decrease of the amount of permanently loaded NPX down to 20 wt% (PEDOT/DS) and 32 wt% (PEDOT/CIO₄).

Acknowledgements

The authors are grateful to the National Science Centre in Poland for financing the research in the framework of Sonata (2016/23/D/ST5/01306). This publication has emanated from research conducted with the financial support of Science Foundation Ireland (SFI) and is co-funded under the European Regional Development Fund under Grant Number 13/RC/2073. This project has received funding from the European Union's Horizon 2020 research and innovation programme under the Marie Skłodowska-Curie grant agreement No 713690. The authors acknowledge the facilities and scientific and technical assistance of the Centre for Microscopy & Imaging at the National University of Ireland Galway, a facility that is funded by NUIG and the Irish Government's Programme for Research in Third Level Institutions, Cycles 4 and 5, National Development Plan 2007-2013.

Declarations of interest:

none

Literature

- [1] A. V. Akkuratov, P.A. Troshin, Conjugated polymers with benzothiadiazole, benzoxadiazole, and benzotriazole moieties as promising semiconductor materials for organic solar cells, *Polym. Sci. Ser. B.* 56 (2014) 414–442. doi:10.1134/S1560090414040010.
- [2] V.A. Kostianovskii, D.K. Susarova, P.A. Troshin, Synthesis of novel conjugated polymers comprising modified cyclopentadithiophene units in the main chain, *High Perform. Polym.* 29 (2017) 670–676. doi:10.1177/0954008317697804.
- [3] P. Zassowski, P. Ledwon, A. Kurowska, A.P. Herman, M. Lapkowski, V. Cherpak, Z. Hotra, P. Turyk, K. Ivaniuk, P. Stakhira, G. Sych, D. Volyniuk, J.V. Grazulevicius, 1,3,5-Triazine and carbazole derivatives for OLED applications, *Dye. Pigment.* 149 (2018) 804–811. doi:10.1016/j.dyepig.2017.11.040.
- [4] P. Zassowski, P. Ledwon, A. Kurowska, A.P. Herman, T. Jarosz, M. Lapkowski, V. Cherpak, P. Stakhira, L. Peciulyte, D. Volyniuk, J.V. Grazulevicius, Efficient synthesis and structural effects of ambipolar carbazole derivatives, *Synth. Met.* 223 (2017) 1–11. doi:10.1016/j.synthmet.2016.11.015.
- [5] P.M. Beaujuge, J.R. Reynolds, Color control in π -conjugated organic polymers for use in electrochromic devices, *Chem. Rev.* 110 (2010) 268–320. doi:10.1021/cr900129a.
- [6] T. Jarosz, A. Brzeczek, K. Walczak, M. Lapkowski, W. Domagala, Multielectrochromism of redox states of thin electropolymerised films of poly(3-dodecylpyrrole) involving a black coloured state, *Electrochim. Acta.* 137 (2014) 595–601. doi:10.1016/j.electacta.2014.06.018.
- [7] D. Svirskis, J. Travas-Sejdic, A. Rodgers, S. Garg, Electrochemically controlled drug delivery based on intrinsically conducting polymers., *J. Control. Release.* 146 (2010) 6–15. doi:10.1016/j.jconrel.2010.03.023.
- [8] T.F. Otero, J.G. Martinez, J. Arias-Pardilla, Biomimetic electrochemistry from conducting polymers. A review: Artificial muscles, smart membranes, smart drug delivery and computer/neuron interfaces, *Electrochim. Acta.* 84 (2012) 112–128. doi:10.1016/j.electacta.2012.03.097.
- [9] D. Esrafilzadeh, J.M. Razal, S.E. Moulton, E.M. Stewart, G.G. Wallace, Multifunctional conducting fibres with electrically controlled release of ciprofloxacin, *J. Control. Release.* 169 (2013) 313–320. doi:10.1016/j.jconrel.2013.01.022.
- [10] K. Krukiewicz, A. Stokfisz, J.K. Zak, Two approaches to the model drug immobilization into conjugated polymer matrix., *Mater. Sci. Eng. C. Mater. Biol. Appl.* 54 (2015) 176–181. doi:10.1016/j.msec.2015.05.017.
- [11] R. Wadhwa, C.F. Lagenaur, X.T. Cui, Electrochemically controlled release of dexamethasone from conducting polymer polypyrrole coated electrode, *J. Control. Release.* 110 (2006) 531–541. doi:10.1016/j.jconrel.2005.10.027.
- [12] M. Asplund, C. Boehler, T. Stieglitz, Anti-inflammatory polymer electrodes for glial scar treatment: bringing the conceptual idea to future results, *Front. Neuroeng.* 7 (2014). doi:10.3389/fneng.2014.00009.
- [13] K. Krukiewicz, M. Cichy, P. Ruszkowski, R. Turczyn, T. Jarosz, J.K. Zak, M. Lapkowski, B. Bednarczyk-Cwynar, Betulin-loaded PEDOT films for regional chemotherapy, *Mater. Sci. Eng. C.* 73 (2017) 611–615.

doi:10.1016/j.msec.2016.12.115.

- [14] N. Alizadeh, E. Shamaeli, Electrochemically controlled release of anticancer drug methotrexate using nanostructured polypyrrole modified with cetylpyridinium: Release kinetics investigation, *Electrochim. Acta.* 130 (2014) 488–496. doi:10.1016/j.electacta.2014.03.055.
- [15] K. Krukiewicz, J.K. Zak, Conjugated polymers as robust carriers for controlled delivery of anti-inflammatory drugs, *J. Mater. Sci.* 49 (2014) 5738–5745. doi:10.1007/s10853-014-8292-2.
- [16] W. Domagala, D. Palutkiewicz, D. Cortizo-Lacalle, A.L. Kanibolotsky, P.J. Skabara, Redox doping behaviour of poly(3,4-ethylenedithiophene) - The counterion effect, *Opt. Mater. (Amst).* 33 (2011) 1405–1409. doi:10.1016/j.optmat.2011.02.030.
- [17] R. Balint, N.J. Cassidy, S.H. Cartmell, Conductive polymers: Towards a smart biomaterial for tissue engineering, *Acta Biomater.* 10 (2014) 2341–2353. doi:10.1016/j.actbio.2014.02.015.
- [18] U. Páramo-García, J.G. Ibanez, N. Batina, Electrochemical modulation of the thickness of polypyrrole films by using different anionic dopants, *Int. J. Electrochem. Sci.* 6 (2011) 5172–5188.
- [19] Q. Zeng, K. Xia, B. Sun, Y. Yin, T. Wu, M.S. Humayun, Electrodeposited Iridium Oxide on Platinum Nanocones for Improving Neural Stimulation Microelectrodes, *Electrochim. Acta.* 237 (2017) 152–159. doi:10.1016/j.electacta.2017.03.213.
- [20] C. Vallejo-Giraldo, K. Krukiewicz, I. Calaresu, J. Zhu, M. Palma, M. Fernandez-Yague, B.W. McDowell, N. Peixoto, N. Farid, G. O'Connor, L. Ballerini, A. Pandit, M.J.P. Biggs, Attenuated Glial Reactivity on Topographically Functionalized Poly(3,4-Ethylenedioxythiophene):P-Toluene Sulfonate (PEDOT:PTS) Neuroelectrodes Fabricated by Microimprint Lithography, *Small.* 14 (2018) 1800863. doi:10.1002/sml.201800863.
- [21] K. Krukiewicz, M. Chudy, C. Vallejo-Giraldo, M. Skorupa, D. Więclawska, R. Turczyn, M. Biggs, Fractal form PEDOT/Au assemblies as thin-film neural interface materials, *Biomed. Mater.* 13 (2018) 54102. <http://stacks.iop.org/1748-605X/13/i=5/a=054102>.
- [22] V. Castagnola, E. Descamps, A. Lecestre, L. Dahan, J. Remaud, L.G. Nowak, C. Bergaud, Parylene-based flexible neural probes with PEDOT coated surface for brain stimulation and recording, *Biosens. Bioelectron.* 67 (2015) 450–457. doi:10.1016/j.bios.2014.09.004.
- [23] L. Jin, T. Wang, Z.Q. Feng, M.K. Leach, J. Wu, S. Mo, Q. Jiang, A facile approach for the fabrication of core-shell PEDOT nanofiber mats with superior mechanical properties and biocompatibility, *J. Mater. Chem. B.* 1 (2013) 1818–1825. doi:10.1039/c3tb00448a.
- [24] F. Pires, Q. Ferreira, C.A.V. Rodrigues, J. Morgado, F.C. Ferreira, Neural stem cell differentiation by electrical stimulation using a cross-linked PEDOT substrate: Expanding the use of biocompatible conjugated conductive polymers for neural tissue engineering, *Biochim. Biophys. Acta.* 1850 (2015) 1158–1168. doi:10.1016/j.bbagen.2015.01.020.
- [25] S. Wang, S. Guan, J. Xu, W. Li, D. Ge, C. Sun, T. Liu, X. Ma, Neural stem cell proliferation and differentiation in the conductive PEDOT-HA/Cs/Gel scaffold for

- neural tissue engineering, *Biomater. Sci.* 5 (2017) 2024–2034.
doi:10.1039/C7BM00633K.
- [26] K. Krukiewicz, P. Zawisza, A.P. Herman, R. Turczyn, S. Boncel, J.K. Zak, An electrically controlled drug delivery system based on conducting poly(3,4-ethylenedioxythiophene) matrix, *Bioelectrochemistry*. 108 (2016) 13–20.
doi:10.1016/j.bioelechem.2015.11.002.
- [27] P. Fattahi, G. Yang, G. Kim, M.R. Abidian, A review of organic and inorganic biomaterials for neural interfaces, *Adv. Mater.* 26 (2014) 1846–1885.
doi:10.1002/adma.201304496.
- [28] S. Khan, M. Ul-Islam, M.W. Ullah, M. Israr, J.H. Jang, J.K. Park, Nano-gold assisted highly conducting and biocompatible bacterial cellulose-PEDOT:PSS films for biology-device interface applications, *Int. J. Biol. Macromol.* 107 (2018) 865–873.
doi:10.1016/j.ijbiomac.2017.09.064.
- [29] R.A. Green, R.T. Hassarati, L. Bouchinet, C.S. Lee, G.L.M. Cheong, J.F. Yu, C.W. Dodds, G.J. Suaning, L.A. Poole-Warren, N.H. Lovell, Substrate dependent stability of conducting polymer coatings on medical electrodes, *Biomaterials*. 33 (2012) 5875–5886. doi:10.1016/j.biomaterials.2012.05.017.
- [30] S.A. Spanninga, D.C. Martin, Z. Chen, Effect of anionic hydration on counterion incorporation in poly(3,4-ethylenedioxythiophene): An X-ray photoelectron spectroscopy study, *J. Phys. Chem. C*. 114 (2010) 14998–15004.
doi:10.1021/jp104592n.
- [31] J.R. Mishic, M.R. Fisch, The size and flexibility of grown sodium dodecyl sulfate micelles in aqueous sodium chloride solutions, *J. Chem. Phys.* 92 (1990) 3222–3229.
doi:10.1063/1.457872.
- [32] C.D. Bruce, M.L. Berkowitz, L. Perera, M.D.E. Forbes, Molecular dynamics simulation of sodium dodecyl sulfate micelle in water: Micellar structural characteristics and counterion distribution, *J. Phys. Chem. B*. 106 (2002) 3788–3793.
doi:10.1021/jp013616z.
- [33] N. Alizadeh, E. Shamaeli, M. Fazili, Online Spectroscopic Monitoring of Drug Release Kinetics from Nanostructured Dual-Stimuli-Responsive Conducting Polymer, *Pharm. Res.* 34 (2017) 113–120. doi:10.1007/s11095-016-2044-8.
- [34] E. Shamaeli, N. Alizadeh, Kinetic studies of electrochemically controlled release of salicylate from nanostructure conducting molecularly imprinted polymer, *Electrochim. Acta*. 114 (2013) 409–415. doi:10.1016/j.electacta.2013.10.119.
- [35] N. Soltani, N. Tavakkoli, Z.S. Mosavimanesh, F. Davar, Electrochemical determination of naproxen in the presence of acetaminophen using a carbon paste electrode modified with activated carbon nanoparticles, *Comptes Rendus Chim.* 21 (2018) 54–60.
doi:10.1016/j.crci.2017.11.007.
- [36] A.L. Haag, I. Nagai, B. Lennox, P. Grütter, Characterization of a gold coated cantilever surface for biosensing applications, *EPJ Tech. Instrum.* 2 (2015) 1.
doi:10.1140/epjti/s40485-014-0011-5.
- [37] D. Plausinaitisa, A. Pulmanasa, M. Waskaasb, R. Raudonisa, V. Daujotisa, Piezoelectric resonator and drag force study of the properties of an interfacial hexafluorophosphate solution layer at gold electrode surface, *Electrochim. Acta*. 109 (2013) 756–765. doi:10.1016/j.electacta.2013.07.169.

- [38] S.A. Spanninga, D.C. Martin, Z. Chen, X-ray photoelectron spectroscopy study of counterion incorporation in poly(3,4-ethylenedioxythiophene) (PEDOT) 2: Polyanion effect, toluenesulfonate, and small anions, *J. Phys. Chem. C.* 114 (2010) 14992–14997. doi:10.1021/jp104591d.
- [39] W. Kunz, J. Henle, B.W. Ninham, “Zur Lehre von der Wirkung der Salze” (about the science of the effect of salts): Franz Hofmeister’s historical papers, *Curr. Opin. Colloid Interface Sci.* 9 (2004) 19–37. doi:10.1016/j.cocis.2004.05.005.
- [40] Y. Zhang, P.S. Cremer, Interactions between macromolecules and ions: the Hofmeister series, *Curr. Opin. Chem. Biol.* 10 (2006) 658–663. doi:10.1016/j.cbpa.2006.09.020.
- [41] D. Gugała-Fekner, J. Nieszporek, D. Sieńko, Adsorption of anionic surfactant at the electrode- NaClO_4 solution interface, *Monatshefte Fur Chemie.* 146 (2015) 541–545. doi:10.1007/s00706-014-1382-7.
- [42] B.A. Abd-El-Nabey, O.A. Abdullatef, G.A. El-Naggar, E.A. Matter, R.M. Salman, Effect of tween 80 surfactant on the electropolymerization and corrosion performance of polyaniline on mild steel, *Int. J. Electrochem. Sci.* 11 (2016) 2721–2733. doi:10.20964/110402721.
- [43] S.F. Cogan, Neural Stimulation and Recording Electrodes, *Annu. Rev. Biomed. Eng.* 10 (2008) 275–309. doi:10.1146/annurev.bioeng.10.061807.160518.
- [44] P.M.C. J.B. Fallon, *Neurobionics: The Biomedical Engineering of Neural Prostheses*, Wiley-Blackwell, New Jersey, 2016. doi:10.1002/9781118816028.
- [45] D.C. Martin, G.G. Malliaras, Interfacing Electronic and Ionic Charge Transport in Bioelectronics, *ChemElectroChem.* 3 (2016) 686–688. doi:10.1002/celec.201500555.
- [46] S.M. Richardson-Burns, J.L. Hendricks, B. Foster, L.K. Povlich, D.H. Kim, D.C. Martin, Polymerization of the conducting polymer poly(3,4-ethylenedioxythiophene) (PEDOT) around living neural cells, *Biomaterials.* 28 (2007) 1539–1552. doi:10.1016/j.biomaterials.2006.11.026.
- [47] R. Ansari Khalkhali, W.E. Price, G.G. Wallace, Quartz crystal microbalance studies of the effect of solution temperature on the ion-exchange properties of polypyrrole conducting electroactive polymers, *React. Funct. Polym.* 56 (2003) 141–146. doi:10.1016/S1381-5148(03)00055-5.
- [48] P.M. Dzięwoński, M. Grzeszczuk, Impact of the electrochemical porosity and chemical composition on the lithium ion exchange behavior of polypyrroles (ClO_4^- , TOS-, TFSI-) prepared electrochemically in propylene carbonate. Comparative EQCM, EIS and CV studies, *J. Phys. Chem. B.* 114 (2010) 7158–7171. doi:10.1021/jp100796a.
- [49] A. Jubert, M.L. Legarto, N.E. Massa, L.L. Tévez, N.B. Okulik, Vibrational and theoretical studies of non-steroidal anti-inflammatory drugs Ibuprofen [2-(4-isobutylphenyl)propionic acid]; Naproxen [6-methoxy- α -methyl-2-naphthalene acetic acid] and Tolmetin acids [1-methyl-5-(4-methylbenzoyl)-1H-pyrrole-2-acetic acid], *J. Mol. Struct.* 783 (2006) 34–51. doi:10.1016/j.molstruc.2005.08.018.
- [50] C. Coletta, Z. Cui, A. Dazzi, J.M. Guigner, S. Néron, J.L. Marignier, S. Remita, A pulsed electron beam synthesis of PEDOT conducting polymers by using sulfate radicals as oxidizing species, *Radiat. Phys. Chem.* 126 (2016) 21–31. doi:10.1016/j.radphyschem.2016.05.003.
- [51] Z. Cui, C. Coletta, R. Rebois, S. Baiz, M. Gervais, F. Goubard, P.H. Aubert, A. Dazzi, S. Remita, Radiation-induced reduction-polymerization route for the synthesis of

- PEDOT conducting polymers, *Radiat. Phys. Chem.* 119 (2016) 157–166.
doi:10.1016/j.radphyschem.2015.10.011.
- [52] C. Kvarnström, H. Neugebauer, S. Blomquist, H.J. Ahonen, J. Kankare, A. Ivaska, N.S. Sariciftci, In situ FTIR spectroelectrochemical characterization of poly(3,4-ethylenedioxythiophene) films, *Synth. Met.* 101 (1999) 66. doi:10.1016/S0379-6779(98)01133-3.
- [53] K. Krukiewicz, T. Jarosz, A.P. Herman, R. Turczyn, S. Boncel, J.K. Zak, The effect of solvent on the synthesis and physicochemical properties of poly(3,4-ethylenedioxythiophene), *Synth. Met.* 217 (2016) 231–236.
doi:10.1016/j.synthmet.2016.04.005.
- [54] A. Kaynak, Effect of synthesis parameters on the surface morphology of conducting polypyrrole films, *Mater. Res. Bull.* 32 (1997) 271–285. doi:10.1016/S0025-5408(96)00200-0.
- [55] C. Zhou, Z. Liu, Y. Yan, X. Du, Y.W. Mai, S. Ringer, Electro-synthesis of novel nanostructured PEDOT films and their application as catalyst support, *Nanoscale Res. Lett.* 6 (2011) 364. doi:10.1186/1556-276X-6-364.
- [56] T. Nie, J.K. Xu, L.M. Lu, K.X. Zhang, L. Bai, Y.P. Wen, Electroactive species-doped poly(3,4-ethylenedioxythiophene) films: Enhanced sensitivity for electrochemical simultaneous determination of vitamins B2, B6 and C, *Biosens. Bioelectron.* 50 (2013) 244–250. doi:10.1016/j.bios.2013.06.057.
- [57] M. Mumtaz, E. Ibarboure, C. Labrugère, E. Cloutet, H. Cramail, Synthesis of PEDOT Nano-objects Using Poly(vinyl alcohol)-Based Reactive Stabilizers in Aqueous Dispersion, *Macromolecules.* 41 (2008) 8964–8970. doi:10.1021/ma801856h.
- [58] Y. Gao, L. Zhao, C. Li, G. Shi, Electrosynthesis of poly(3,4-ethylenedioxythiophene) microcups in the aqueous solution of LiClO₄ and tri(ethylene glycol), *Polymer (Guildf).* 47 (2006) 4953–4958. doi:10.1016/j.polymer.2006.05.021.
- [59] H. Okamoto, T. Kotaka, Effect of counter ions in electrochemical polymerization media on the structure and responses of the product polyaniline films: III. Structure and properties of polyaniline films prepared via electrochemical polymerization, *Polymer (Guildf).* 40 (1999) 407–417. doi:10.1016/S0032-3861(98)00248-1.
- [60] J. Wang, Y. Xu, X. Chen, X. Du, X. Li, Effect of Doping Ions on Electrochemical Capacitance Properties of Polypyrrole Films, *Acta Phys. - Chim. Sin.* 23 (2007) 299–304. doi:10.1016/S1872-1508(07)60023-0.
- [61] J. Yang, D.H. Kim, J.L. Hendricks, M. Leach, R. Northey, D.C. Martin, Ordered surfactant-templated poly(3,4-ethylenedioxythiophene) (PEDOT) conducting polymer on microfabricated neural probes, *Acta Biomater.* 1 (2005) 125–136.
doi:10.1016/j.actbio.2004.09.006.
- [62] J. Sui, L. Zhang, J. Travas-Sejdic, P.A. Kilmartin, Synthesis of Poly(3,4-ethylenedioxythiophene) hollow spheres in CTAB/DBS - Mixed surfactant solutions, *Macromol. Symp.* 290 (2010) 107–114. doi:10.1002/masy.201050412.
- [63] T.D.Y. Kozai, A.S. Jaquins-Gerstl, A.L. Vazquez, A.C. Michael, X.T. Cui, Brain tissue responses to neural implants impact signal sensitivity and intervention strategies, *ACS Chem. Neurosci.* 6 (2015) 48–67. doi:10.1021/cn500256e.
- [64] E.J. Howe, B.O. Okesola, D.K. Smith, Self-assembled sorbitol-derived supramolecular hydrogels for the controlled encapsulation and release of active pharmaceutical

- ingredients, *Chem. Commun.* 51 (2015) 7451–7454. doi:10.1039/c5cc01868d.
- [65] E. Shamaeli, N. Alizadeh, Nanostructured biocompatible thermal/electrical stimuli-responsive biopolymer-doped polypyrrole for controlled release of chlorpromazine: Kinetics studies, *Int. J. Pharm.* 472 (2014) 327–338. doi:10.1016/j.ijpharm.2014.06.036.
- [66] A.S. Hutchison, T.W. Lewis, S.E. Moulton, G.M. Spinks, G.G. Wallace, Development of polypyrrole-based electromechanical actuators, *Synth. Met.* 113 (2000) 121–127. doi:10.1016/S0379-6779(00)00190-9.
- [67] A. Zykwincka, W. Domagala, M. Lapkowski, ESR spectroelectrochemistry of poly(3,4-ethylenedioxythiophene) (PEDOT), *Electrochem. Commun.* 5 (2003) 603–608. doi:10.1016/S1388-2481(03)00132-2.
- [68] C. Boehler, M. Asplund, A detailed insight into drug delivery from PEDOT based on analytical methods: Effects and side effects, *J. Biomed. Mater. Res. - Part A.* 103 (2015) 1200–1207. doi:10.1002/jbm.a.35252.
- [69] C. Boehler, C. Kleber, N. Martini, Y. Xie, I. Dryg, T. Stieglitz, U.G. Hofmann, M. Asplund, Actively controlled release of Dexamethasone from neural microelectrodes in a chronic in vivo study, *Biomaterials.* 129 (2017) 176–187. doi:10.1016/j.biomaterials.2017.03.019.

Figures & captions

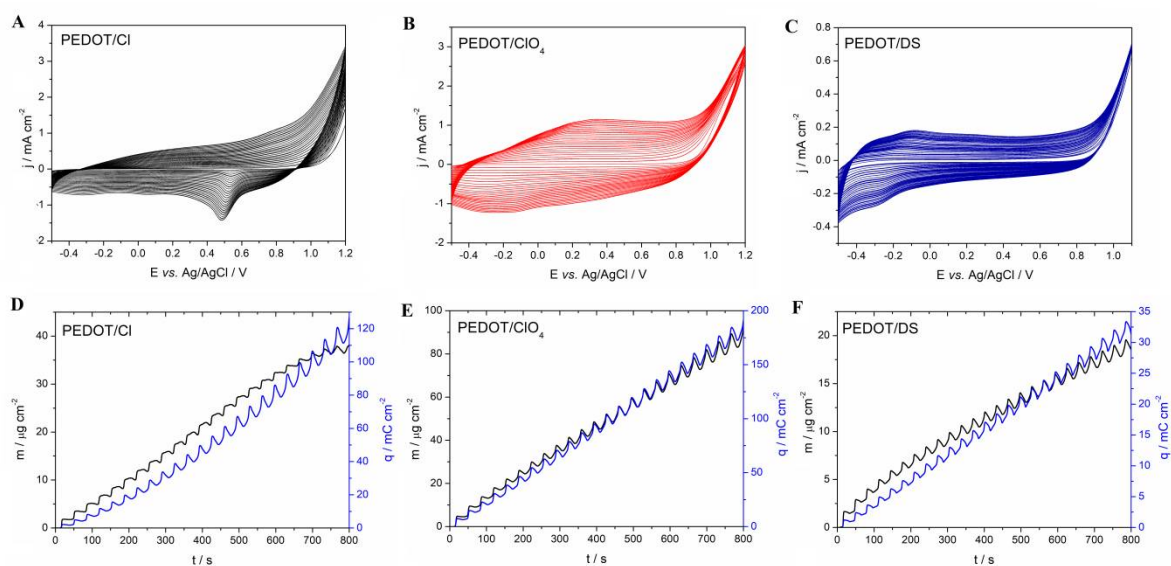


Figure 1. Cyclic voltammograms of the process of electrochemical polymerization of 10 mM EDOT in the presence of 0.1 M KCl (A), 0.1 M LiClO₄ (B) and 0.1 M DS (C); the change in mass (black line) and charge density (blue line) as a function of time for PEDOT/Ci (D), PEDOT/CiO₄ (E) and PEDOT/DS (F).

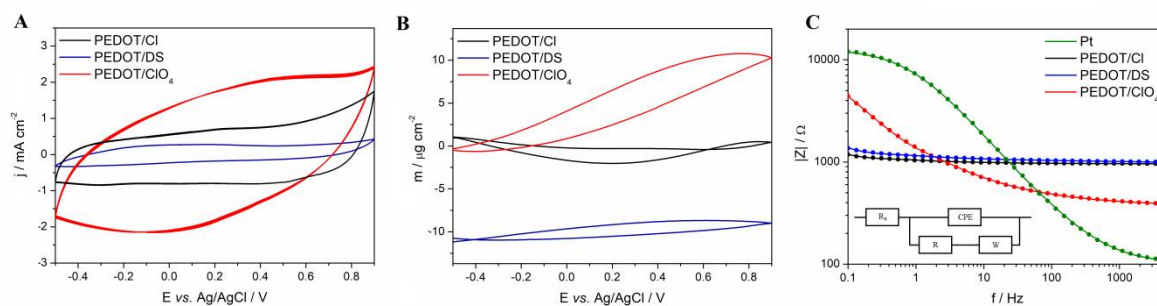


Figure 2. Cyclic voltammograms (A) and the corresponding changes in mass (B) of PEDOT/Ci (black line), PEDOT/CiO₄ (red line) and PEDOT/DS (blue line); impedance module vs. frequency (C) for PEDOT/Ci (black line), PEDOT/CiO₄ (red line), PEDOT/DS (blue line) and bare platinum (green line), with the equivalent circuit presented as the inset.

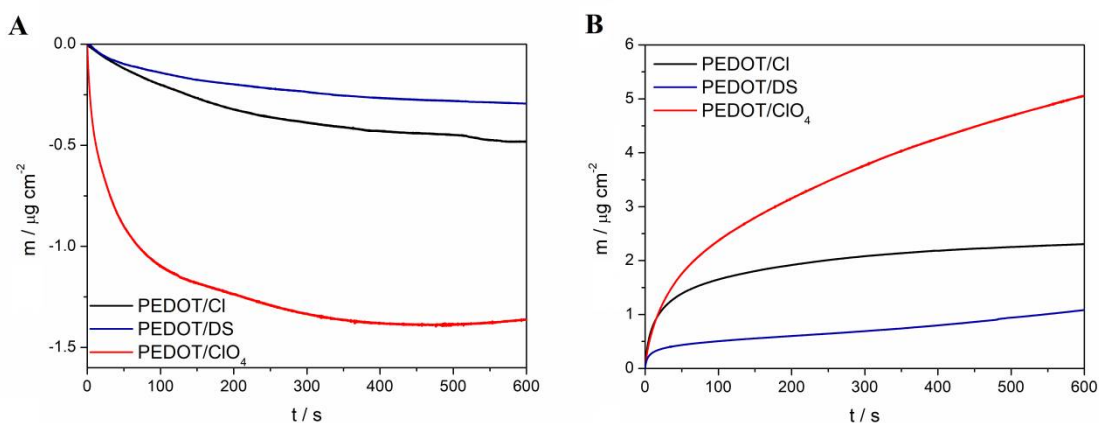


Figure 3. Mass changes of matrices: PEDOT/Cl (black line), PEDOT/ ClO_4 (red line) and PEDOT/DS (blue line) collected during the release of a primary dopant (A) and drug loading (B) stages

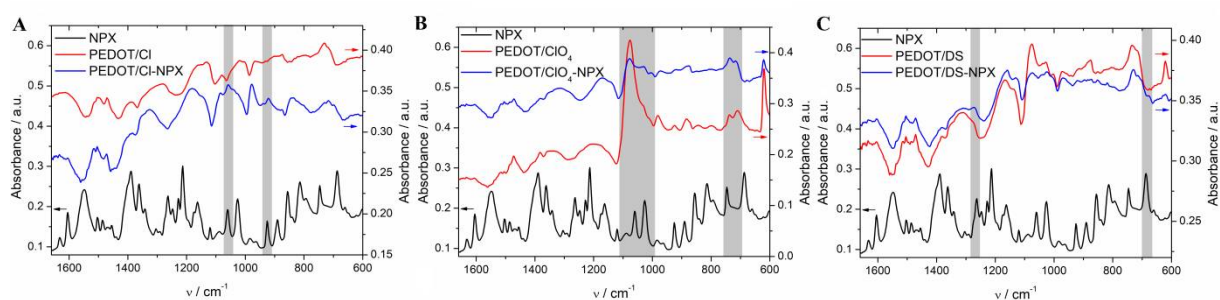


Figure 4. FTIR spectra of NPX (black line), PEDOT (red line) and NPX-loaded PEDOT (blue line) for the conducting polymer matrices electropolymerized in the presence of different primary dopants: Cl^- (A), ClO_4^- (B) and DS^- (C).

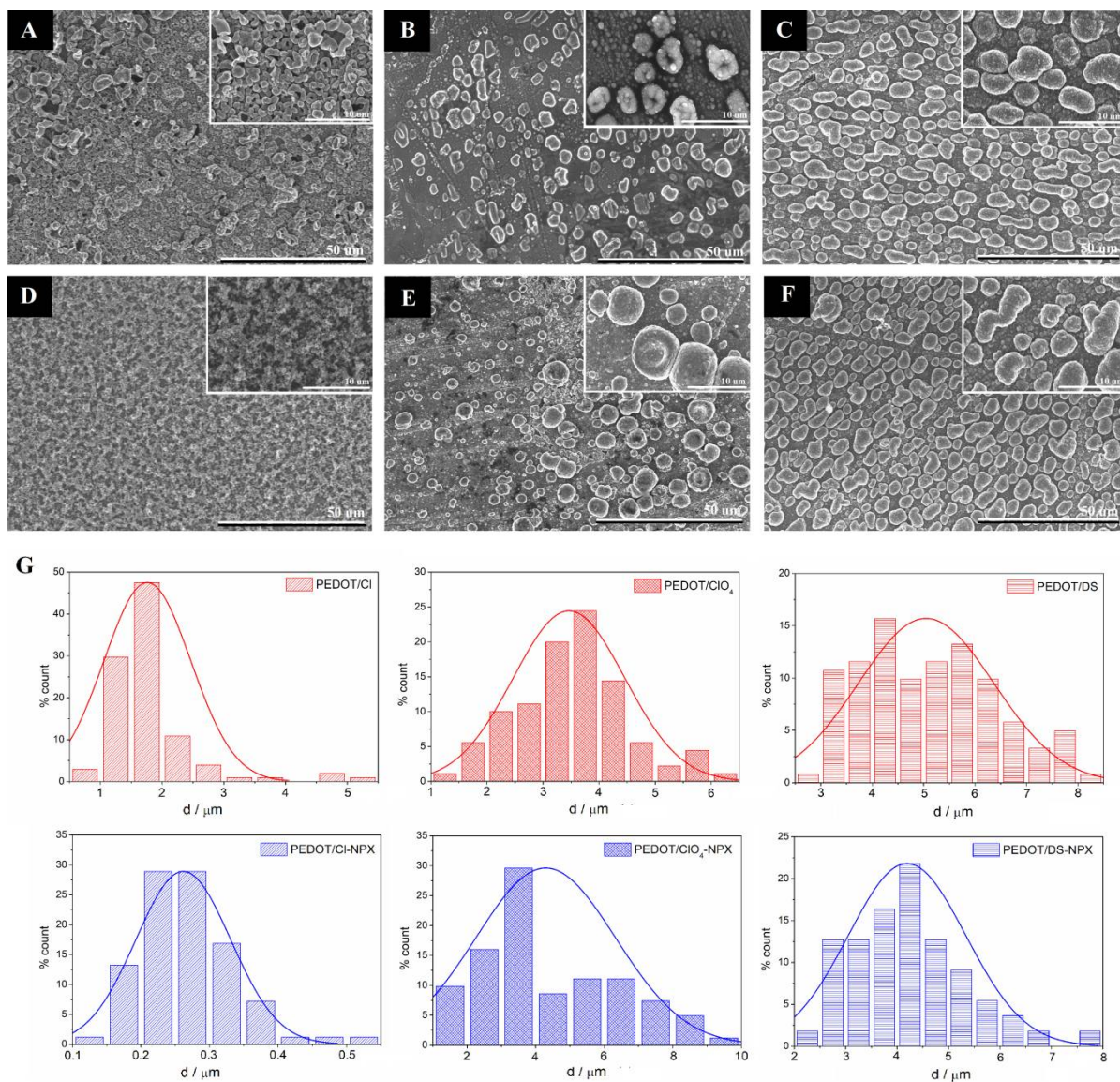


Figure 5. SEM images of the pristine (A-C) and NPX-loaded (D-F) PEDOT/Cl (A,D), PEDOT/ClO₄ (B,E) and PEDOT/DS (C,F) matrices (scale bar of 50 μm); the insets show higher magnification images (scale bar of 10 μm); histograms (G) show the diameter of features present on the pristine and drug-loaded PEDOT matrices.

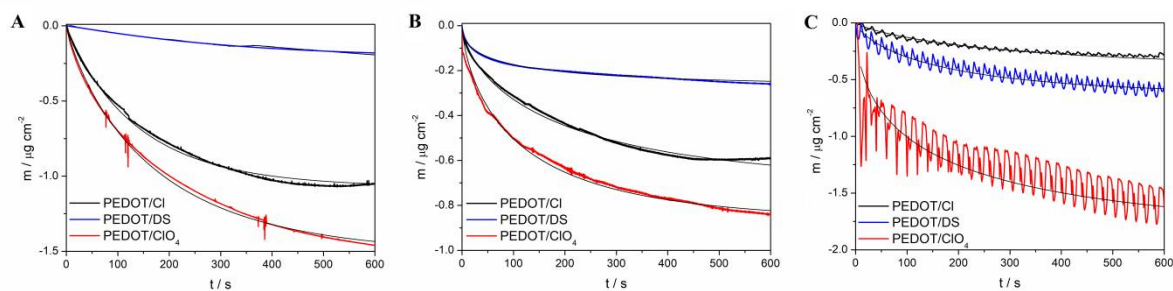


Figure 6. Representative mass vs. time curves of the three release modes: spontaneous (A), chronoamperometric (B) and cyclic voltammetric (C) for PEDOT/Cl (black line), PEDOT/ClO₄ (red line) and PEDOT/DS (blue line) matrices. Thin black lines represent the corresponding fitted curves calculated by means of Avrami's equation.

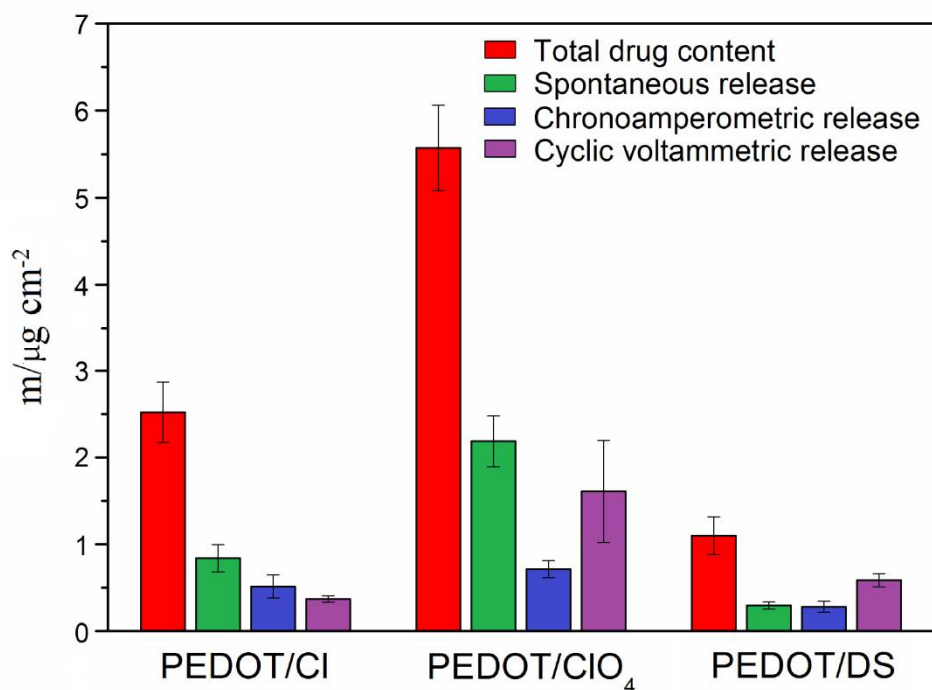


Figure 7. Mass of NPX loaded and released from PEDOT/Cl, PEDOT/ClO₄ and PEDOT/DS with the use of the spontaneous, chronoamperometric and cyclic voltammetric types of release. The values are expressed as a mean of five measurements \pm standard error.

Tables

Table 1. Mass changes and ion exchange capacities of PEDOT/Cl, PEDOT/CIO₄ and PEDOT/DS based on the cyclic oxidation and reduction of matrices. The values are expressed as a mean of five measurements ± standard error.

	PEDOT/Cl	PEDOT/CIO₄	PEDOT/DS
Mass change of matrix during a single CV, $\mu\text{g cm}^{-2}$	2.95 ± 0.02	12.09 ± 0.38	2.57 ± 0.21
Ion exchange capacity, $\mu\text{mole cm}^{-2}$	0.083 ± 0.001	0.122 ± 0.003	0.010 ± 0.001

Table 2. Mass changes of PEDOT/Cl, PEDOT/CIO₄ and PEDOT/DS in the processes of the removal of primary dopant (600 s) and drug loading (600 s), as well as the total drug content. The values are expressed as a mean of five measurements ± standard error.

	PEDOT/Cl	PEDOT/CIO₄	PEDOT/DS
Polymer mass, $\mu\text{g cm}^{-2}$	42.07 ± 2.53	103.45 ± 10.09	17.49 ± 0.58
Mass decrease due to the removal of dopant, $\mu\text{g cm}^{-2}$	0.50 ± 0.08	1.63 ± 0.30	0.25 ± 0.04
Mass increase due to drug loading, $\mu\text{g cm}^{-2}$	2.52 ± 0.35	5.57 ± 0.49	1.10 ± 0.22
Drug content, wt%	5.71 ± 0.91	5.18 ± 0.71	5.99 ± 1.28

Table 3. NPX release efficiency of PEDOT/Cl, PEDOT/CIO₄ and PEDOT/DS with the use of spontaneous, chronoamperometric and cyclic voltammetric types of release. The values are expressed as a mean of five measurements ± standard error. The values in brackets describe the wt% of the amount of drug released through a specific method with respect to the total drug content.

	PEDOT/Cl	PEDOT/CIO₄	PEDOT/DS
Spontaneous release, $\mu\text{g cm}^{-2}$	0.84 ± 0.16 (33 %)	2.19 ± 0.29 (39 %)	0.30 ± 0.04 (27 %)
Chronoamperometric release, $\mu\text{g cm}^{-2}$	0.51 ± 0.13 (20 %)	0.71 ± 0.10 (13 %)	0.28 ± 0.06 (25 %)
Cyclic voltammetric release, $\mu\text{g cm}^{-2}$	0.37 ± 0.04 (15 %)	1.61 ± 0.59 (29 %)	0.58 ± 0.08 (53 %)
NPX loaded permanently, wt%	47 % (CA) 52% (CV)	48 % (CA) 32 % (CV)	48% (CA) 20 % (CV)